MECHANISM OF LOAD TRANSFER-CRACK WIDTH RELATION IN JPCP: INFLUENCE OF COARSE AGGREGATE PROPERTIES

By

Elin A. Jensen, Graduate Student Research Assistant
Will Hansen, Associate Professor

Department of Civil Engineering at University of Michigan
2350 Hayward, Ann Arbor, MI 48109

ABSTRACT

Aggregate interlock was analyzed from continuous measurements of crack deflections for concrete slabs-on-grade subjected to wheel loading up to 40kN using a large-scale slab test system. These results show that aggregate interlock is comprised of at least three significant components: (1) an initial slack or gap between crack surfaces, which exists prior to loading, (2) a sliding of the adjacent crack surfaces, and (3) an in-plane dilation of the crack if unrestrained, otherwise build-up of normal force. The significance of dilation forces increases with crack width and approaches the crack shear load in magnitude for large crack widths (e.g. 2.5mm). These mechanisms vary with crack width and roughness. Roughness in turn is controlled by timing of cracking (i.e. PCC strength), coarse aggregate type and size. Tough and large-size aggregate had reduced slack and sliding and maintained high load transfer.

INTRODUCTION

The mechanism responsible for transferring stresses across a crack in jointed plain concrete pavements, JPCP's, from the loaded to the unloaded side is rather complex. The mechanism is influenced by crack width, aggregate type and size, time of crack initiation, slab thickness, slab length, slab temperature, slab-base friction factor, and magnitude and repetition of load (e.g. Colley and Humphrey, 1967; Nowlen, 1968; Bruinsma et al., 1995; Abdel-Maksoud et al., 1998; and Buch et al., 2000)

Field Observations on Load Transfer versus Crack Width

A recent field study in Michigan of jointed reinforced concrete pavements, JRCP's, found that the surface crack width was a good indicator of the load transfer efficiency, LTE. The age of the JRCP's ranged between 10 and 14 years (Hansen et al., 1998.) These results, shown in figure 1, suggest that long-term field load transfer may decrease rapidly for crack widths exceeding about 0.6 mm and that the aggregate interlock is lost at about 1 mm. These results are in good agreement with findings by other investigators (e.g. Colley and Humphrey, 1967; and Buch et al., 2000). In the field study by Hansen et al.(1998), it was also apparent that crack spalling was more prevalent with larger crack widths.

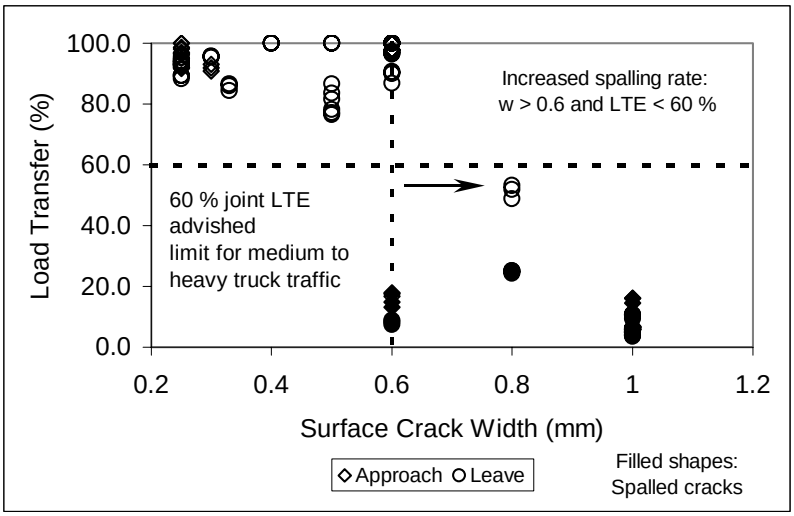

Figure 1 Load transfer versus crack width based on field observations from six different JRPC's (Hansen et al., 1998).

Aggregate Interlock

When a crack is formed in normal strength concrete, the majority of the coarse aggregate particles remain embedded in the mortar on either side of the crack. The strength of the aggregate-mortar interface zone is lower than that of the coarse aggregate resulting in cracking around the aggregate forming a rough and irregular crack surface. However, if the coarse aggregate is weaker than that of the interface zone and the mortar, the crack will penetrate through the aggregate resulting in a straight and smoother crack surface (e.g. Vervuurt, 1997; Mohammed and Hansen, 1999; and Jensen and Hansen, 2001).

Aggregate interlock provides shear resistance along the fractured surface. Pittman (1996) suggested that as load is applied, the loaded side of a crack or joint deflects a certain distance before touching the unloaded crack face. This initial deflection is denoted as crack slack. As the load is increased, the loaded and the unloaded slab may deflect at the same rate, which indicates high crack face bearing force and friction resulting in good load transfer. Consider another situation with small aggregates (or fractured aggregates) and smooth vertical crack face. In this case the initial deflection of the loaded slab side will tend to increase due to higher slack and during subsequent deflection the two crack faces may slide relative to each other.

In this paper, the slack and the slippage that occurs in the crack during wheel loading is determined along with the in-plane crack dilation restraining force that is developed during loading and crack deflection. Once the mechanisms controlling the aggregate interlock properties across a crack surface is better understood and can be quantified for different coarse aggregate types and top size, an improved material-based model can be developed for predicting aggregate interlock in JPCP's.

Current Aggregate Interlock Models

In finite element models, the aggregate interlock is commonly modeled as a series of vertical linear springs adjoining two adjacent slabs. Each discontinuity (joint or crack) is given a unique value representing a given load transfer, measured or assumed (e.g. ILLI-SLAB, Tabatabaei, 1977; KENSLABS, Huang, 1985; and EVERFE, Davids et al., 1998. For tight cracks bending stresses can be transferred as well, however, this effect is often ignored (Nishizawa et al., 1997.) These spring models are based on a linear elastic solution of the edge load transfer problem.

Determining the spring stiffness for a given joint or crack can become an elaborate procedure. The accurate aggregate interlock factor is determined through iteration to obtain the best suitable factor for a given load transfer in a particular pavement system.

Many fundamentally different constitutive models have been proposed to describe shear transfer across cracks. Raja and Snyder (1991) summarized the most pertinent models to pavement design. The models have been developed based on a series of different test results, which are likely the main reason for the varying conclusions. The models describe the interlock factor through local and global roughness (Laible et al., 1977), frictional resistance between the two opposing sides (Jimenez et al., 1978), or shear resistance developed through sliding of the aggregate elements over the cement matrix (Bazant and Gambarova, 1980, and Walraven, 1981). These models require detailed information or approximation of the crack roughness. Currently, the two-phase model proposed by Walraven (1981) is available in EVERFE (Davids et al., 1998).

The drawback of these aggregate interlock models is the scarcity of data to accurately predict the effect of coarse aggregate type and top size for the deflection range that occurs in concrete slabs in the field, and to predict the impact on long-term pavement performance.

EXPERIMENTAL DESIGN

A laboratory large-scale slab testing system was used in order to control the timing of cracking and the development of load versus deflection for a wide range of crack widths. Furthermore, the slab testing does not reflect field conditions causing intermittent or permanent loss of joint or crack support, (i.e. curling or warping,) and effects from seasonal temperature cycles, precipitation, and freeze-thaw cycles.

Large-Scale Slab Testing System

The system is shown in figure 2. As illustrated the slab is placed on a full depth foundation, connected to a horizontal reaction frame through twelve 30-mm threaded steel rods embedded in the concrete and attached to a loading plate. The slab is fixed to the frame at one end; the other end is movable by means of an actuator with a load cell capacity of 1100 kN in compression and 550 kN in tension. At midslab a crack is created at a given age (around 7 days) by sawing a 70 mm surface notch and pulling the slab apart with the horizontal actuator. After the crack has been created the aggregate interlock is determined at a wide range in crack widths starting at around 0.3 mm and ending at about 2.5 mm. During testing the crack width is maintained at constant crack width through a joint displacement feedback control. The wheel load was

simulated as a cycling load with a maximum magnitude of 40 kN at a rate of 3 Hz. For each crack width a total of about 300,000 load cycles is used to evaluate the response. A 300-mm circular loading plate was used on the approach crack to simulate an equivalent single axle tire load.

A 250 mm thick PCC slab with overall dimensions of 3.0 m by 1.8 m was placed on a typical Michigan highway foundation (i.e. 102 mm open-graded drainage course on a 400 mm thick subbase). The entire test area rested on a sand foundation. Both the base and the subbase were compacted to a minimum of 95 percent of the optimum density as verified by Density In-Place (nuclear) test. The base and subbase extends about 0.50 m from the slab edge in all directions. The composite modulus of subgrade reaction was determined before the slab was placed.

Timing of Slab Cracking

The crack was created when the concrete splitting tensile strength had exceeded 70 percent of the expected 28-day strength. This occurs typically between 7 to 10 days after casting. Table 1 shows that the 70 percent strength limit was exceeded at the time of crack initiation. A full width and depth crack was created from the surface notch at midslab. Subjecting the slab to a horizontal displacement, controlled at one end, created the crack. The displacement at the other slab end was constant. The surface crack width was measured using a clip-gauge with a travel of ±4 mm. The slab displacement and load were transferred through the 12 rods, which were embedded about 300 mm into the slab.

Deflection Instrumentation

The vertical frame with actuator is shown at midslab along with the reference beam and the extensometers to measure the deflections on either side of the crack. The vertical deflections were measured using ±4 mm extensometers. The vertical deflections were measured relative to the reference beam that was supported on the slab ends. Figure 3 shows the two extensometers spaced 150 mm on each side of the crack located immediately left of the center of the loading plate. The slab was positioned at a certain crack width as measured by the clip-gauge and a relative crack width measurer.

Slab Testing

The slabs were typically tested at the following crack widths: 0.3, 0.45, 0.6, 0.9, 1.2, 1.6, 2.0 and 2.5 mm. Each crack width was subjected to 100,000 to 300,000 vertical loading cycles. Detailed data collection was performed at predetermined intervals at N = 100, 1000, 5000, 10000, 25000, 50000, … (100000) …300000. Load and deflections were obtained for one hundred loading cycles for detailed evaluation.

Furthermore, the free-edge load-deflection response was obtained after all crack widths had been tested. Free edge response was assumed reached when the crack width had exceeded 5 mm. Determining the slab-base friction factor concluded the test sequence.



Figure 2 Overview of large-scale slab testing system



Figure 3 Close-up of loading and deflection arrangement

Materials

Table 1 and figure 4 list the key aggregate and PCC properties of the investigated concretes. Two aggregate types and two sizes are evaluated. The aggregate types are glacial gravel with LA abrasion value of 22 percent wear and limestone with LA abrasion value of 34 percent wear. The glacial gravel was evaluated for a maximum size of 25 and of 50 mm. Figure 4 shows the grain distribution curves for the three gradations. The large size blend was constructed such that 40 percent of the material was retained on the 25 mm sieve, and 10 percent was retained on the 38 mm sieve. The concrete 28-day compressive strength, splitting tensile strength, and the fracture energy are listed along with the splitting tensile strength at the time of crack initiation. The fracture energy is a measure of the energy required to fully develop a crack (Jensen and Hansen, 2001).

Table 1 Aggregate and concrete properties.

PCC Mix with Aggregate Type	Max. Size (mm)	BSG (g/cm^3)	AC (%)	LA Abrasion (% of wear)	28-day Compressive Strength (MPa)	28-day Split. Tensile Strength (MPa)	Split. Tensile Strength at the time of crack initiation (MPa)	28-day Fracture Energy (N/m)
Glacial Gravel	25	2.58	0.80	22	30.6	2.93	2.33	140
Glacial Gravel	50	2.58	0.80	22	32.8	2.41	2.21	175
Limestone	25	2.61	1.00	34	34.8	2.47	2.17	90

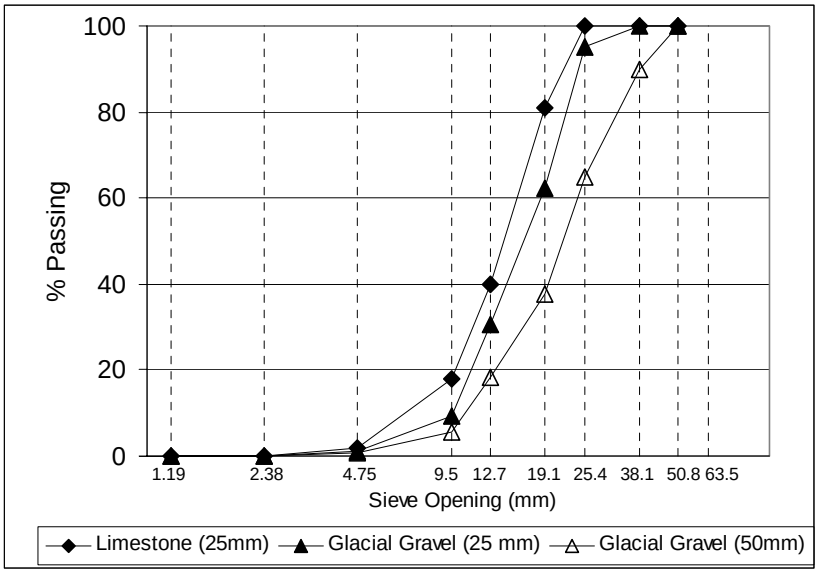

Figure 4 Coarse aggregate gradation curves.

Mix Design

The mix design criteria were employed for a 24 MPa minimum 28-day compressive strength mix containing coarse aggregate with the 25 (or 50) mm maximum aggregate size. The criteria are:

335 kg type I cement per m^3 fresh concrete
5.5 (5.0) percent air in the fresh concrete
1.15 (1.20) relative water content
0.72 (0.80) workability

The relative water content expresses the additional required water over the basic water content to obtain workable fresh concrete. The workability is the volume of the loose coarse aggregate per unit volume of fresh concrete.

RESULTS AND DISCUSSION

Deflection, Load Transfer, and Crack Width

Crack width was found to be the primary factor controlling the slab deflection for any of the aggregates tested, which is in agreement with previously published work (e.g. Colley and Humphrey, 1967; and Nowlen, 1968.) The results are illustrated in figure 5 for three cases, the limestone concrete with 25-mm top size and the glacial gravel concrete for top sizes 25 and 50 mm. The slab peak deflections in this study are greater than typically measured in the field using falling weight deflectometer, FWD. The reason is twofold and due to the unrestrained slab shoulders and the thick layer of embankment (subbase) used in the geotechnical pit for this study. Maximum deflections ranged between 0.6 and 0.8 mm for the three slabs. This factor is not adhered to affect the outcome of this study as a deflection plateau was reached for each crack width tested.

There appears to be three significant stages of load transfer for a slab resting on a foundation. Stage I signifies a tight crack (width < 0.5 mm). A tight crack has nearly 100 percent load transfer, as deflections are the same on either side of the crack. In this stage the effect of aggregate type and top size was found to be small. This is possibly due to the closing pressure that had to be applied across the crack after the crack was first created. As a result of crack closing, prior to testing, a force had to be applied by the horizontal actuator, across the cracked face, to hold the crack tight. This artificial force may have reduced the slab deflections for crack widths up to about 0.5 mm as this is the range where the force is needed. This is shown in figure 6, where the normal force represent the stage where the load transfer and the slab deflections have stabilized as observed from the their relative curves with number of load applications. A constant plateau was reached at any crack width and for all aggregate systems tested after 10,000 to 25,000 cycles. Depending on these curves loading was terminated either after 100,000 or 300,000 cycles. Thus, the load transfer obtained for w = 0.3 and 0.45 mm should be considered with care if included in modeling of aggregate interlock.

Stage II is the range where aggregate interlock plays a primary role. Stage II represents crack width of 0.6 mm to the stage where the aggregates no longer provide shear resistance. In this study, the maximum crack width tested was 2.5 mm. For softer aggregates such as the limestone aggregate used in this study the aggregate interlock is decreasing rapidly with increasing crack width above 0.6 mm consistent with field observations using FWD. The decrease in aggregate interlock is associated with a major decrease in the deflection of the unloaded side and a slight increase in the deflection on the loaded side. It is apparent that only the 50-mm top size material can maintain high level of aggregate interlock for crack widths up to the maximum tested (i.e. 2.0 to 2.5 mm).

The last region indicated in figure 5 is Stage III and it corresponds to crack widths larger than 2.5 mm. This region represents the contribution from the elastic deformation of the foundation.

The load transfer efficiency, LTE, versus crack width is another way of demonstrating the behavior in stages I and II as LTE represent the deflection of the unloaded side of a crack relative to the deflection of the loaded side. This is shown in figure 7. When evaluating the vertical crack face it is clear that the concretes containing glacial gravel obtain a high “ball and socket”

effect due to the many protruding aggregates, rough crack, whereas the concrete containing limestone due to the many cracked aggregates, smooth crack, is void of the effect.

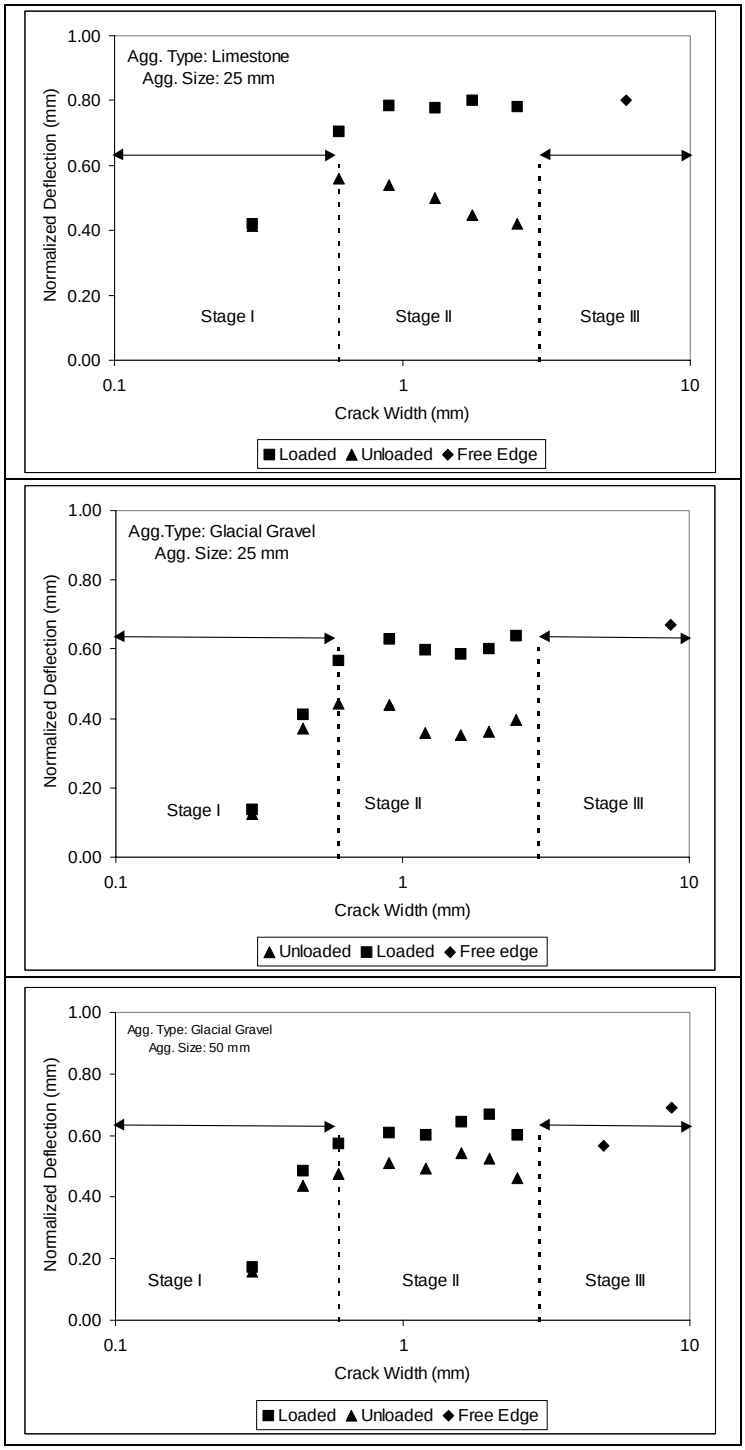

Figure 5 Deflection on the loaded and unloaded slab side versus crack width.

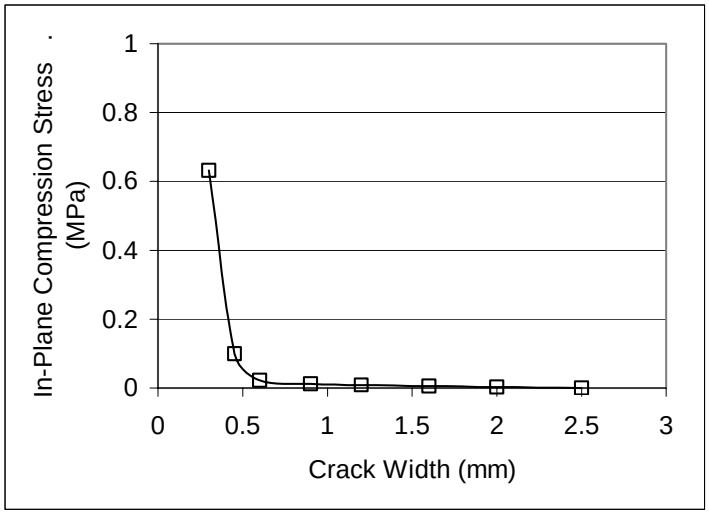

Figure 6 In-plane closing compression stress versus crack width. The compression stress is applied as a joint reaction to maintain and test a tight crack.

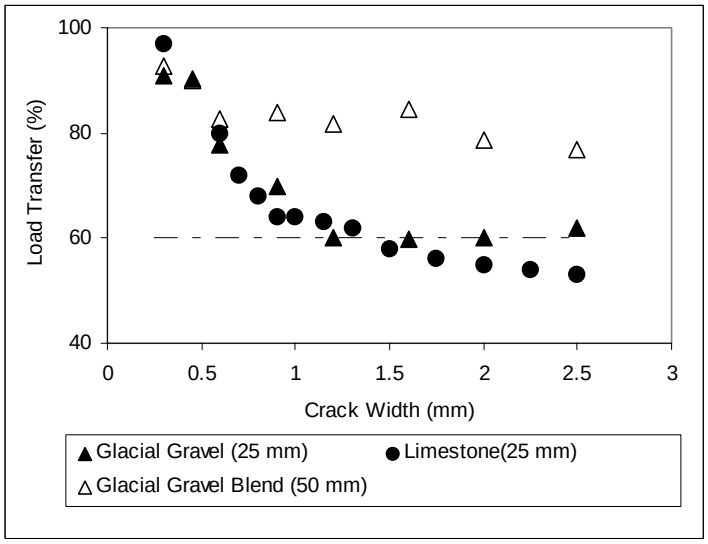

Figure 7 Load transfer versus crack width

Mechanism of Slab Deflection under Wheel Loading

Crack Slack and Sliding

Figure 8 illustrates the development of deflections when the crack is subjected to wheel loading. For the sake of illustration, the deflections have been normalized as described on the figure. Figure 8a shows d_l versus d_u, and figure 8b shows the wheel load versus d_l.

Three different behaviors are observed. For small crack widths the two deflections develop with the same rate, resulting in a 1-1 slope. For increasing crack widths, the unloaded slab segment is not employed before the loaded slab side has deflected a given distance denoted as the slack. However, when the unloaded slab segment is engaged the two sides deflect at an equal rate that results in an 1-1 slope on the second part of the deflection curve. For very large crack widths, in

this case w = 2.0 mm, the loaded side keeps deflecting at a higher rate than the unloaded side, which indicate that the unloaded side is slipping during loading, and this is denoted as slippage. The amount of slack and slippage is dictated by the properties of the crack, crack width and crack roughness.

Figure 8b shows the load versus the deflection of the loaded side. For small crack widths the curves show an almost linear response. For increasing crack widths, the slope of the load-deflection curve becomes steeper as the load increases. This illustrates that the system stiffness increases to maximum at a given load level depending on the crack width. The maximum system stiffness is dictated by the slab and foundation stiffness. Comparing figure 8a and 8b, the maximum system stiffness is reached when the loaded and the unloaded slab segment deflect at the same rate.

a)

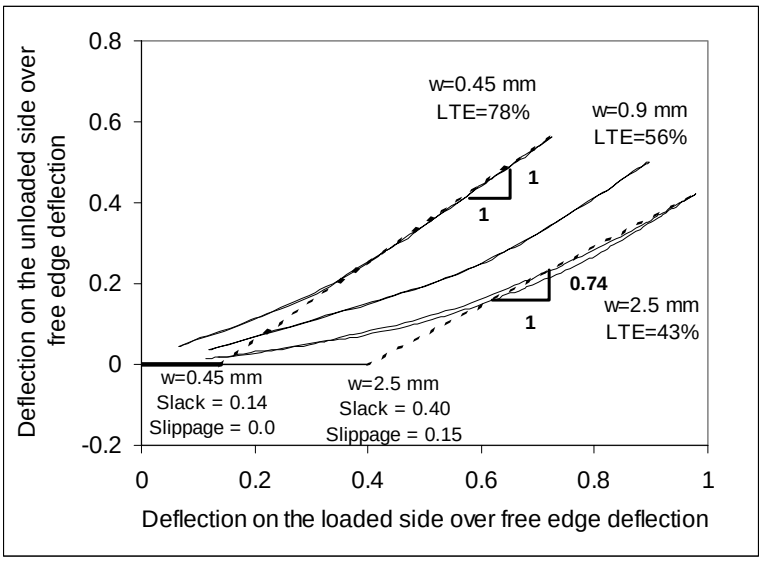

b)

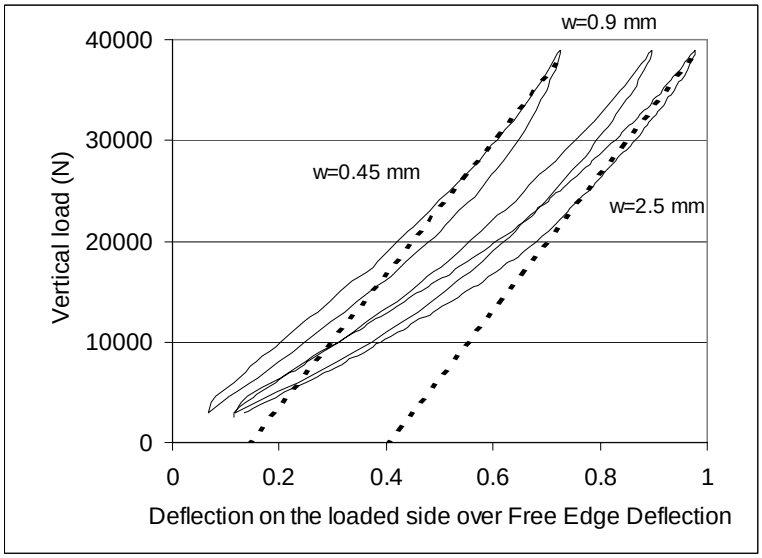

Figure 8 Deflection development under wheel loading.

Crack Dilation

It is well known that concrete cracks can transfer significant amount of shear through aggregate interlock. The shear displacement associated with the crack sliding roughly parallel to the plane of the crack is essential to mobilize shear transfer by aggregate interlock. The shear displacement is accompanied by a displacement in the normal direction (dilation) owing to aggregates projecting across the sliding path. If the crack is restraint from moving, the resistance to dilation is transformed into a normal stress (Divakar et al., 1987). In this laboratory study, the crack width is maintained constant during loading causing a restraining force to act across the crack.

Figure 9 and 10 shows the normal restraining force averaged over the slab width for a limestone and a glacial gravel both with a maximum top-size of 50 mm. The figures show that as the crack is being loaded the normal force increases linearly, and that the build-up of normal forces is proportional to the vertical loading. Second, it is seen that the concrete containing the glacial gravel develops higher normal force as the concrete containing limestone at the same crack widths. The difference in behavior is associated with the difference in slack and sliding between the two concretes. The limestone concrete develops a significant amount of slack, and increasing sliding with increasing crack width. The gravel concrete develops much less slack, but has significant increased sliding even at smaller crack widths. (This will be illustrated in detail in figure 11.)

These findings agree with results reported by Abdel-Maksoud et al. (1998) where the joint behavior was evaluated during completely reversed cyclic loading of cracked concrete specimens. The restraining force observed in this study is smaller than what was observed by Abdel-Maksoud et al. (1998). The reason, in part, is that this study evaluates a concentrated load relative to larger cross section area (3.6 times larger). Currently, work is concentrating on evaluating the "effective" cross section area of the slab, and horizontal crack movement during wheel loading.

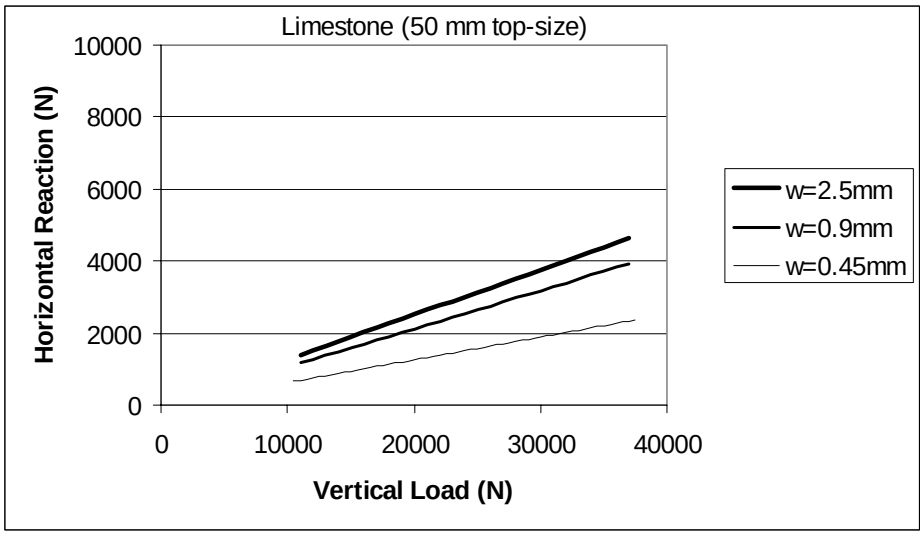

Figure 9 Restraining force versus shear displacement of the crack.

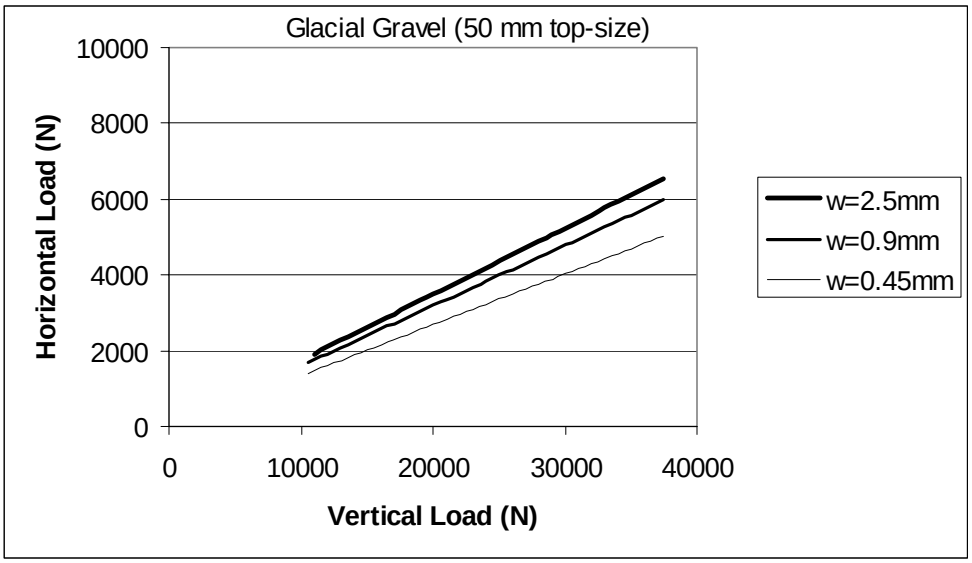

Figure 10 Restraining force versus shear displacement of the crack.

Figure 11 shows the deflections of the loaded slab segment versus the unloaded slab segment for the three evaluated concretes, and for each crack width the slack and the slope of the deflections curves are tabulated. The slippage is indicated through the slope of the later part of the deflection curves. The development of deflections in the three slabs indeed shows aggregate dependent behavior. The concrete containing limestone shows both the developments of slack and slippage for increasing crack widths. The concrete containing glacial gravel develops mainly slack, however it is less than that observed for the limestone concrete, and the slippage remains almost constant for increasing crack widths. For increased maximum aggregate size from 25 to 50 mm for the glacial gravel concrete, the slack decreases.

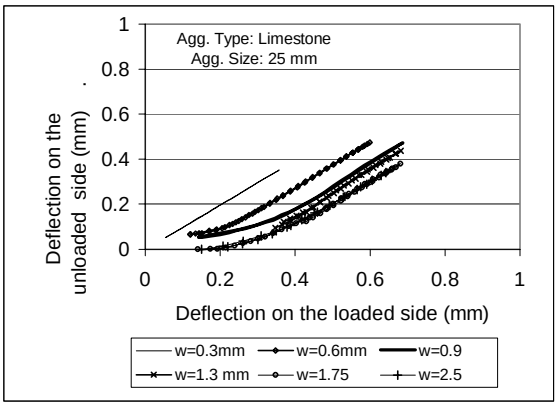

w (mm)	slack (mm)	slope (-)
0.30	0.002	0.99
0.60	0.133	1.00
0.90	0.237	1.00
1.30	0.278	1.00
1.75	0.292	0.95
2.50	0.291	0.96

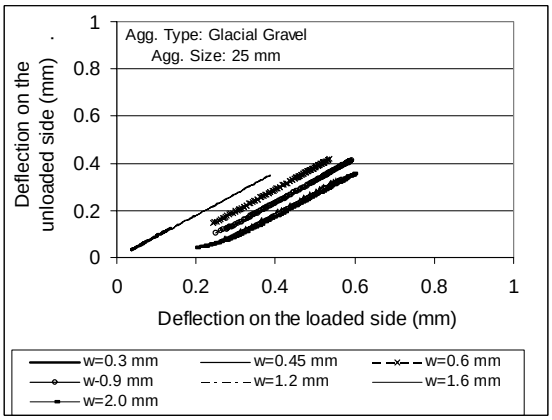

w (mm)	slack (mm)	slope (-)
0.30	0.002	0.92
0.45	0.005	0.92
0.60	0.088	0.93
0.90	0.151	0.93
1.20	0.187	0.90
1.60	0.187	0.90
2.00	0.201	0.90
2.50	0.200	0.90

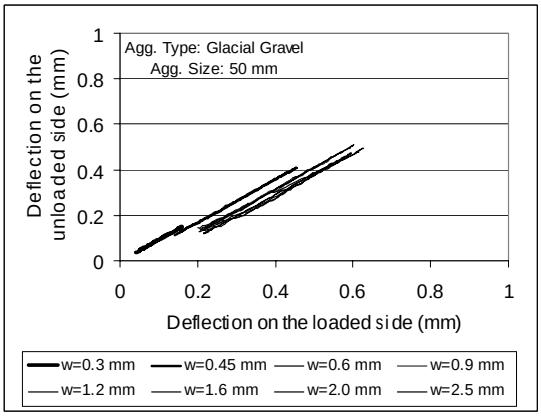

w(mm)	slack (mm)	slope (-)
0.30	0.002	0.94
0.45	0.023	0.95
0.60	0.069	0.95
0.90	0.069	0.95
1.20	0.089	0.93
1.60	0.069	0.95
2.00	0.080	0.90
2.50	0.081	0.89

Figure 11 Deflection on the loaded versus unloaded side for the concretes containing limestone, gravel, and large size gravel.

The difference in the deflection development is contributed to the smoothness of the crack. The crack path of the limestone concrete was significantly smoother than that of the concrete containing glacial gravel. The crack had penetrated the limestone aggregates whereas the crack had developed around glacial gravel. One can compare the crack path of concrete containing glacial gravel to the "ball and socket" effect. The difference in the crack path is mainly controlled by the fracture properties of the concrete and the aggregate hardness. Note the

transverse crack in these slabs was created in tension when the concrete tensile strength had exceeded 70 percent of the 28-day strength, which typically occurred around 7-10 days of age.

Figure 12 shows the combined amount of slack and slippage as the difference between d_l and d_u at peak load versus crack width. The figure shows that the shear displacement increases rapidly for crack widths between 0.3 and 0.6 mm. For larger crack widths, $0.6 \leq w \leq 2.5$ mm, the slack increases at a reduced rate. At w = 2.5 mm, the slack can vary from 0.20 to 0.45 from the concrete containing large size gravel to the concrete containing limestone. For w > 2.5 mm the slack would eventually increase rapidly and asymptotically go towards one.

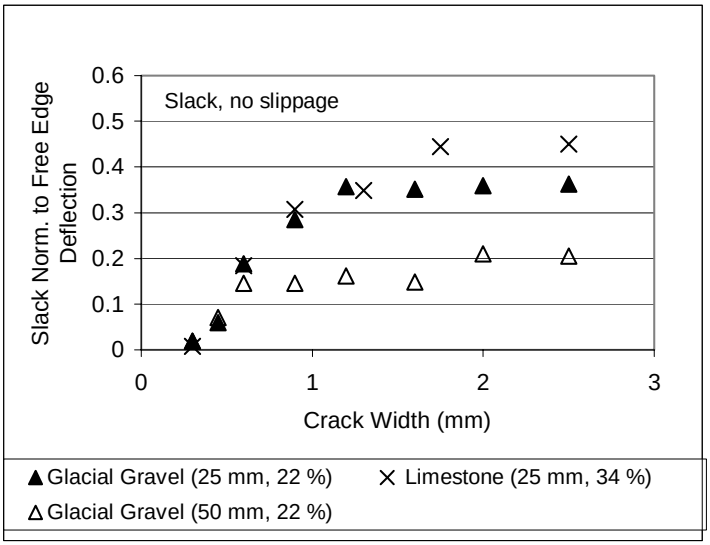

Figure 12 Shear displacement versus crack width

New Model Considerations

The results showed that the slab response to shear loading of a fully developed crack include different mechanisms such as slack, sliding, and dilation. These mechanisms depend on crack width and crack geometry (roughness and tortuosity), and they determine the magnitude of shear and normal forces that develop at the crack surface during wheel loading. An important consideration in model development will be to quantify the key factors that affect the crack roughness. Lets for now just combine these factors into one function, $f_{pcc}()$, that includes the PCC fracture properties, which in turn controls crack roughness and tortuosity. Therefore, the crack shear load, P, and normal load, N, can be written in general as

$$N = f_N (w, \text{slack}, \text{sliding}, f_{pcc}(), P)$$
$$P = f_P (w, \text{slack}, \text{sliding}, f_{pcc}())$$

These two functions are interrelated and govern the constitutive relation at a crack. More work is needed to establish the function form with respect to the major variables.

CONCLUSIONS

The aggregate interlock mechanism was investigated for concretes containing different coarse aggregate types and top sizes from a laboratory investigation of cracked JPCP using a large-scale slab testing system. The major findings are:

- Aggregate interlock is comprised of at least three significant components: (1) an initial slack or gap between crack surfaces, which exists prior to loading, (2) sliding of the adjacent crack surfaces, and (3) in-plane dilation of the crack if unrestrained, otherwise build-up of normal stress.

- The significance of dilation forces increases with crack width and is associated with the sliding and roughness of the crack face. (e.g. 2.5mm).

- These mechanisms vary with crack width and roughness. Roughness in turn is controlled by timing of cracking (i.e. PCC strength), coarse aggregate type and size. Tough and large-size aggregate had reduced slack and sliding and maintained high load transfer.

- Crack width was found to be the controlling parameter of the aggregate interlock, which is in agreement with work presented in the literature.

ACKNOWLEDGEMENT

The authors acknowledge the support from Michigan Department of Transportation (MDOT) as part of the project "Transverse Crack Propagation of JPCP as Related to PCC Toughness." The authors also wish to thank John Staton and David L. Smiley, and the Technical Advisory Group (TAG), MDOT, for their guidance and technical assistance throughout the project. The contents of this paper reflect the views of the authors and do not necessarily reflect the view or the policy of the supporting agency.

REFERENCES

Abdel-Maksoud, M.G., N. Hawkins, and E. Barenberg (1998). Effect of Geometric and mechanical properties of concrete joints on their cyclic shear response. Presented for the 1999 Federal Aviation Administration, Technology Transfer Conference.

Bazant, Z.P., and Gambarova, P. (1980). Rough Cracks in Reinforced Concrete. ASCE, Vol. 106, No. ST4, April 1980, pp. 819-842.

Bruinsma, J.E., Raja, Z.I., Snyder, M.B., and Vandenbosshe (1995). Factors Affecting the Deterioration of Transverse Cracks in JRCP. Final Report, Contract 90-0973, to Michigan Department of Transportation. Michigan State University.

Buch, N., Frabizzio, M.A., and Hiller, J.E. (2000). Factors Affecting Shear Capacity of Transverse Cracks in Jointed Concrete Pavements (JCP). Final report to Michigan Department of Transportation. Michigan State University.

Colley, B.E., and Humphrey, H.A. (1967). Aggregate Interlock at Joints in Concrete Pavements. Highway Research Record 189. National Research Council. pp. 1-18.

Davids, W.G., Turkiyyah, G.M., Mahoney, J.P. (1998). EverFE – Rigid Pavement Three-Dimensional Finite Element Analysus Tool. Transportation Research Record 1629. National Research Council. pp.41-49.

Divakar, M.P., Fafitis, A., Shah, S.P. (1987). Constitutive model for Shear Transfer in Cracked Concrete. Journal of Structural Engineering, Vol 113, No. 5, May, 1987, pp, 1046-1062.

Hansen, W., Definis, A., Jensen, E., Byrum, C.R, Mohamed, A.R., Mohr, P., and Grove, G (1998). Investigation of Transverse Cracking On Michigan PCC Pavements over Open-Graded Drainage Course. Final Report to Michigan Department of Transportation, University of Michigan.

Huang, Y.H. (1985) A Computer Package for Structural Analysis of Concrete Pavements. Proceedings, 3rd International Conference on Concrete Pavement Design and Rehabilitation, Purdue University, pp. 295-307.

Jensen, E.A., and Hansen, W. (2000) Fracture Energy Test for Highway Concrete-Determining the Effect of Coarse Aggregate on Crack Propagation Resistance. Transportation Research Record 1730, pp. 10-16.

Jimenez, R., Gergely, P., and White, R.N. (1978). Shear Transfer Across Cracks in Reinforced Concrete. Report 78-4. Cornell University, Ithaca, N.Y., Aug.

Laible, J.P., White, R.N., and Gergely, P. (1977). Experimental Investigation of Seismic Shear Transfer Across Cracks in Concrete Nuclear Containment Vessels. Reinforced Concrete Structures in Seismic Zones, ACI SP-53, American Concrete Institute, Detroit. pp. 203-226.

Mohammed, A.R., and Hansen, W. (1999). Micromechanical Modeling of Crack-Aggregate Interaction in Concrete Materials. Journal of Cement and Concrete Composites.

Nishizawa, T., Shimeno, S., Komatsubara, A., and Koyanagawa, M. (1997). Load Transfer at Transverse Cracks in Continuously reinforced Concrete Pavement. Proceeding Vol. 3., Sixth International Purdue Conference on Concrete Pavement Design and Materials for High Performance, Purdue University. pp. 125-146.

Nowlen, W.J. (1968) Influence of Aggregate Properties on Effectiveness of Interlock Joints in concrete Pavements. Journal of the PCA, Research and Development Laboratories, Vol. 10., No. 2, May. pp. 2-8.

Pittman, D.W. (1996). Factors Affecting Joint Efficiency of Roller-Compacted Concrete Pavement Joints and Cracks. Transportation Research Board 1525. National Research Council. Washington D.C. pp. 10-20.

Raja, Z.I., and M.B. Snyder (1991) Factors Affecting Deterioration of Transverse Cracks in Jointed Reinforced Concrete Pavements. In Transportation Research Board N0. 1307. National Research Council, Washington D.C., pp. 162-168.

Smith, K.D., Perskin, D.G., Darter, M.I., Mueller, A.L., and Carpenter, S.H. (1990) Performance of Jointed Pavements," Vol. 1, Evaluation of Concrete Pavement Performance and Design Features. Federal Highway Administration, FHWA-RD-89-136, March 1990.

Tabatabaie, A.M. (1977). Structural Analysis of Concrete Pavement Joints. Ph.D. Thesis, University of Illinois.

Vervuurt, A. (1997) Interface Fracture in Concrete. Ph.D. Thesis. CIP-GEGEVENS KONINKLIJKE BIBILOTHEEK DEN HAAG.

Walraven, J.C. (1981). Fundamental Analysis of Aggregate Interlock. Journal of the Structural Division, ASCE, Vol. 107, No. 11, Nov. pp. 2245-2270.